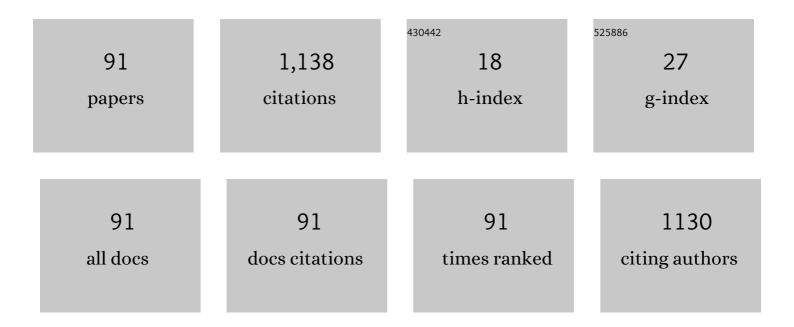
## Yoshio Yamamoto

List of Publications by Year in descending order

Source: https://exaly.com/author-pdf/5435881/publications.pdf Version: 2024-02-01



#	Article	IF	CITATIONS
1	Immunohistochemical colocalization of TREK-1, TREK-2 and TRAAK with TRP channels in the trigeminal ganglion cells. Neuroscience Letters, 2009, 454, 129-133.	1.0	58
2	TASK-1, TASK-2, TASK-3 and TRAAK immunoreactivities in the rat carotid body. Brain Research, 2002, 950, 304-307.	1.1	53
3	Altered production of nitric oxide and reactive oxygen species in rat nodose ganglion neurons during acute hypoxia. Brain Research, 2003, 961, 1-9.	1.1	44
4	Seasonal Changes in Subcellular Structures of Leydig and Sertoli Cells in the Japanese Black Bear, Ursus thibetanus japonicus Archives of Histology and Cytology, 1997, 60, 225-234.	0.2	42
5	Morphology of aging lung in F344/N rat: Alveolar size, connective tissue, and smooth muscle cell markers. The Anatomical Record, 2003, 272A, 538-547.	2.3	37
6	Seasonal Changes in the Immunolocalization of Steroidogenic Enzymes in the Testes of the Japanese Black Bear (Ursus thibetanus japonicus) Journal of Veterinary Medical Science, 1997, 59, 521-529.	0.3	36
7	Hypoxia induces production of nitric oxide and reactive oxygen species in glomus cells of rat carotid body. Cell and Tissue Research, 2006, 325, 3-11.	1.5	35
8	Distribution of TRPV1―and TRPV2â€immunoreactive afferent nerve endings in rat trachea. Journal of Anatomy, 2007, 211, 775-783.	0.9	32
9	Morphological and quantitative study of the intrinsic nerve plexuses of the canine trachea as revealed by immunohistochemical staining of protein gene product 9.5. , 1998, 250, 438-447.		28
10	Stimulation of dopamine D2â€iike receptors in the lumbosacral defaecation centre causes propulsive colorectal contractions in rats. Journal of Physiology, 2016, 594, 4339-4350.	1.3	26
11	Distribution of neurotensin-containing neurons in the central nervous system of the pigeon and the chicken. , 1996, 375, 187-211.		25
12	Calretinin Immunoreactive Nerve Endings in the Trachea and Bronchi of the Rat Journal of Veterinary Medical Science, 1999, 61, 267-269.	0.3	25
13	Age-related changes in sensory and secretomotor nerve endings in the larynx of F344/N rat. Archives of Gerontology and Geriatrics, 2003, 36, 173-183.	1.4	25
14	Distribution of neurotensin-containing neurons in the central nervous system of the dog. Journal of Comparative Neurology, 1995, 353, 67-88.	0.9	23
15	Morphology of P2X3-immunoreactive nerve endings in the rat laryngeal mucosa. Histochemistry and Cell Biology, 2016, 145, 131-146.	0.8	23
16	Dopamine D1 Receptor Immunoreactivity on Fine Processes of GFAP-Positive Astrocytes in the Substantia Nigra Pars Reticulata of Adult Mouse. Frontiers in Neuroanatomy, 2017, 11, 3.	0.9	20
17	Vagal Afferent Nerve Endings in the Trachealis Muscle of the Dog Archives of Histology and Cytology, 1994, 57, 473-480.	0.2	19
18	Morphological study of the vagal afferent nerve endings in the laryngeal mucosa of the dog. Annals of Anatomy, 1997, 179, 65-73.	1.0	19

Υοςηιο Υαμαμοτο

#	Article	IF	CITATIONS
19	Calbindin D28k-immunoreactive afferent nerve endings in the laryngeal mucosa. The Anatomical Record, 2000, 259, 237-247.	2.3	19
20	Immunolocalization of VR1 and VRL1 in rat larynx. Autonomic Neuroscience: Basic and Clinical, 2005, 117, 62-65.	1.4	19
21	Differences in respiratory changes and Fos expression in the ventrolateral medulla of rats exposed to hypoxia, hypercapnia, and hypercapnic hypoxia. Respiratory Physiology and Neurobiology, 2015, 215, 64-72.	0.7	19
22	Short-term Hypoxia Increases Tyrosine Hydroxylase Immunoreactivity in Rat Carotid Body. Journal of Histochemistry and Cytochemistry, 2010, 58, 839-846.	1.3	18
23	Immunohistochemical localization of tryptophan hydroxylase and serotonin transporter in the carotid body of the rat. Histochemistry and Cell Biology, 2013, 140, 147-155.	0.8	18
24	Cellular distribution of oxygen sensor candidates?Oxidases, cytochromes, K+-channels?in the carotid body. Microscopy Research and Technique, 2002, 59, 234-242.	1.2	16
25	Glutamate- and GABA-mediated neuron–satellite cell interaction in nodose ganglia as revealed by intracellular calcium imaging. Histochemistry and Cell Biology, 2010, 134, 13-22.	0.8	16
26	Vesicular glutamate transporter 2-immunoreactive afferent nerve terminals in the carotid body of the rat. Cell and Tissue Research, 2014, 358, 271-275.	1.5	16
27	Nerve plexuses in the trachea and extrapulmonary bronchi of the rat. Archives of Histology and Cytology, 2004, 67, 41-55.	0.2	15
28	Immunohistochemical analysis for G protein in the olfactory organs of soft-shelled turtle, <i>Pelodiscus sinensis</i> . Journal of Veterinary Medical Science, 2016, 78, 245-250.	0.3	15
29	Apocrine sweat glands in the circumanal glands of the dog. , 1998, 252, 403-412.		14
30	Immunohistochemical localization of carbonic anhydrase isozymes in the rat carotid body. Journal of Anatomy, 2003, 202, 573-577.	0.9	14
31	Sympathetic and sensory innervation of small intensely fluorescent (SIF) cells in rat superior cervical ganglion. Cell and Tissue Research, 2015, 359, 441-451.	1.5	14
32	Three-dimensional architectures of P2X2-/P2X3-immunoreactive afferent nerve terminals in the rat carotid body as revealed by confocal laser scanning microscopy. Histochemistry and Cell Biology, 2016, 146, 479-488.	0.8	14
33	Increased total volume and dopamine β-hydroxylase immunoreactivity of carotid body in spontaneously hypertensive rats. Autonomic Neuroscience: Basic and Clinical, 2012, 169, 49-55.	1.4	13
34	Serotonergic projections to the ventral respiratory column from raphe nuclei in rats. Neuroscience Research, 2019, 143, 20-30.	1.0	13
35	Specific Anti-peptide Antibody to β Subunit of Chicken Thyrotropin: Production and Characterization. Journal of Reproduction and Development, 2002, 48, 197-204.	0.5	13
36	Localization of Neuropeptides in Endocrine Cells of the Chicken Thymus Journal of Veterinary Medical Science, 1997, 59, 601-603.	0.3	12

Υοςηίο Υληματο

#	Article	IF	CITATIONS
37	Circumanal glands of the dog: A new classification and cell degeneration. , 1998, 250, 251-267.		11
38	Laryngeal endocrine cells: topographic distribution and adaptation to chronic hypercapnic hypoxia. Histochemistry and Cell Biology, 2000, 114, 277-282.	0.8	11
39	Heterogeneous expression of TASK-3 and TRAAK in rat paraganglionic cells. Histochemistry and Cell Biology, 2003, 120, 335-339.	0.8	11
40	Differential Expression of Histochemical Characteristics in the Developing Olfactory Receptor Cells in a Flatfish, Barfin Flounder ( <i>Verasper moseri</i> ). Journal of Veterinary Medical Science, 2004, 66, 1609-1611.	0.3	11
41	Morphology and chemical characteristics of subepithelial laminar nerve endings in the rat epiglottic mucosa. Histochemistry and Cell Biology, 2012, 138, 25-39.	0.8	11
42	Short-term Hypoxia Transiently Increases Dopamine $\hat{I}^2$ -Hydroxylase Immunoreactivity in Glomus Cells of the Rat Carotid Body. Journal of Histochemistry and Cytochemistry, 2013, 61, 55-62.	1.3	11
43	Tenascin-C Expression in Equine Tendon-derived Cells During Proliferation and Migration. Journal of Equine Science, 2013, 24, 17-23.	0.2	11
44	Immunohistochemical localization of dopamine D2 receptor in the rat carotid body. Acta Histochemica, 2015, 117, 784-789.	0.9	11
45	Morphological study on the olfactory systems of the snapping turtle, Chelydra serpentina. Tissue and Cell, 2016, 48, 145-151.	1.0	11
46	Topographic distribution of serotonin-immunoreactive urethral endocrine cells and their relationship with calcitonin gene-related peptide-immunoreactive nerves in male rats. Acta Histochemica, 2017, 119, 78-83.	0.9	11
47	Morphogenesis of the Olfactory Pit in a Flatfish, Barfin Flounder (Verasper moseri). Journal of Veterinary Medical Science, 2004, 66, 1275-1278.	0.3	10
48	Immunohistochemical Distribution of Inwardly Rectifying K+ Channels in the Medulla Oblongata of the Rat. Journal of Veterinary Medical Science, 2008, 70, 265-271.	0.3	10
49	Sympathetic regulation of vascular tone via noradrenaline and serotonin in the rat carotid body as revealed by intracellular calcium imaging. Brain Research, 2015, 1596, 126-135.	1.1	10
50	Neurochemical markers in the nervous plexus of the canine glottis. Journal of the Autonomic Nervous System, 1998, 71, 111-119.	1.9	8
51	Expression of ENaC subunits in sensory nerve endings in the rat larynx. Neuroscience Letters, 2006, 402, 227-232.	1.0	8
52	Morphology of <scp>GNAT</scp> 3â€immunoreactive chemosensory cells in the rat larynx. Journal of Anatomy, 2019, 234, 149-164.	0.9	8
53	Vesicular nucleotide transporterâ€immunoreactive type I cells associated with P2X3â€immunoreactive nerve endings in the rat carotid body. Journal of Comparative Neurology, 2020, 528, 1486-1501.	0.9	8
54	Morphology of P2X3â€immunoreactive nerve endings in the rat tracheal mucosa. Journal of Comparative Neurology, 2018, 526, 550-566.	0.9	8

Υοςηιο Υαμαμοτο

#	Article	IF	CITATIONS
55	Pathology of Interdigital Glands in a Wild Japanese Serow (Capricornis crispus) Infected with Parapoxvirus Journal of Veterinary Medical Science, 1997, 59, 1063-1065.	0.3	7
56	Serotonin-mediated modulation of hypoxia-induced intracellular calcium responses in glomus cells isolated from rat carotid body. Neuroscience Letters, 2015, 597, 149-153.	1.0	7
57	<small>L</small> -Lysine Attenuates Hepatic Steatosis in Senescence-Accelerated Mouse Prone 8 Mice. Journal of Nutritional Science and Vitaminology, 2018, 64, 192-199.	0.2	7
58	Neurotensin-Containing Endocrine Cells and Neurotensin Receptor mRNA-Expressing Epithelial Cells in the Chicken Thymus Archives of Histology and Cytology, 1996, 59, 197-203.	0.2	6
59	Distribution and morphology of baroreceptors in the rat carotid sinus as revealed by immunohistochemistry for P2X3 purinoceptors. Histochemistry and Cell Biology, 2019, 151, 161-173.	0.8	6
60	Olecranon Lesions Caused by Onchocerca skrjabini in Wild Japanese Serows (Capricornis crispus) Journal of Veterinary Medical Science, 1997, 59, 387-390.	0.3	5
61	Innervation of NADPH diaphorase-containing neurons correlated with acetylcholinesterase, tyrosine hydroxylase, and neuropeptides in the pigeon cloaca. Journal of Anatomy, 2001, 198, 181-188.	0.9	5
62	Differences in tyrosine hydroxylase expression after short-term hypoxia, hypercapnia or hypercapnic hypoxia in rat carotid body. Respiratory Physiology and Neurobiology, 2010, 173, 95-100.	0.7	5
63	Localization of eNOS in the Olfactory Epithelium of the Rat. Journal of Veterinary Medical Science, 2011, 73, 423-430.	0.3	5
64	GABA-mediated modulation of ATP-induced intracellular calcium responses in nodose ganglion neurons of the rat. Neuroscience Letters, 2015, 584, 168-172.	1.0	5
65	Immunohistochemical characterization of brush cells in the rat larynx. Journal of Molecular Histology, 2018, 49, 63-73.	1.0	5
66	Expression of Fos protein in brainstem after application of l-menthol to the rat nasal mucosa. Neuroscience Letters, 2008, 435, 246-250.	1.0	4
67	Hypoxia-induced increases in serotonin-immunoreactive nerve fibers in the medulla oblongata of the rat. Acta Histochemica, 2016, 118, 806-817.	0.9	4
68	Morphology and chemical characteristics of taste buds associated with P2X3â€immunoreactive afferent nerve endings in the rat incisive papilla. Journal of Anatomy, 2022, 240, 688-699.	0.9	4
69	Structure of the perilobular sheath of the deep proventricular gland of the chicken: presence and possible role of myofibroblasts. Cell and Tissue Research, 1996, 285, 109-117.	1.5	3
70	Age-related changes in immunoreactivity for dopamine β-hydroxylase in carotid body glomus cells in spontaneously hypertensive rats. Autonomic Neuroscience: Basic and Clinical, 2017, 205, 50-56.	1.4	3
71	Immunohistochemical analysis of the development of olfactory organs in two species of turtles Pelodiscus sinensis and Mauremys reevesii. Acta Histochemica, 2018, 120, 806-813.	0.9	3
72	Vesicular glutamate transporter 2-immunoreactive afferent nerve terminals in rat carotid sinus baroreceptors. Acta Histochemica, 2020, 122, 151469.	0.9	3

Υοςηίο Υληματο

#	Article	IF	CITATIONS
73	Distribution of pH regulators in the rat laryngeal nerve: the spatial relationship between Na+/HCO3â^' cotransporters and Na+/H+ exchanger type 3. Neuroscience Letters, 2004, 368, 127-129.	1.0	2
74	Morphological Development and Expression of Neurotrophin Receptors in the Laryngeal Sensory Corpuscles. Anatomical Record, 2011, 294, 694-705.	0.8	2
75	Short-term hypoxia increases phosphorylated tyrosine hydroxylase at Ser31 and Ser40 in rat carotid body. Respiratory Physiology and Neurobiology, 2013, 185, 543-546.	0.7	2
76	Transient appearance of the epithelial invagination in the olfactory pit of chick embryos. Journal of Veterinary Medical Science, 2015, 77, 89-93.	0.3	2
77	Serotonin-mediated modulation of acetylcholine-induced intracellular calcium responses in chromaffin cells isolated from the rat adrenal medulla. Neuroscience Letters, 2017, 644, 114-120.	1.0	2
78	Multicoding in neural information transfer suggested by mathematical analysis of the frequency-dependent synaptic plasticity in vivo. Scientific Reports, 2020, 10, 13974.	1.6	2
79	Immunolocalization of Tandem Pore Domain K+ Channels in the Rat Carotid Body. , 2006, 580, 9-14.		2
80	Morphology of the Glomerular Nerve Endings in the Dorsal Nasal Ligament of the Dog Archives of Histology and Cytology, 2000, 63, 467-472.	0.2	1
81	Parvalbumin in cortical epithelial cells of the pigeon thymus. Journal of Anatomy, 2000, 196, 305-311.	0.9	1
82	Time-dependent changes in cardiorespiratory functions of anesthetized rats exposed to sustained hypoxia. Autonomic Neuroscience: Basic and Clinical, 2018, 212, 1-9.	1.4	1
83	Distribution and morphology of <scp>P2X3</scp> â€immunoreactive subserosal afferent nerve endings in the rat gastric antrum. Journal of Comparative Neurology, 2021, 529, 2014-2028.	0.9	1
84	GluN2A- and GluN2B-immunoreactive type I cells attached to vesicular glutamate transporter 2-immunoreactive afferent nerve terminals of the rat carotid body. Histochemistry and Cell Biology, 2021, 155, 719-726.	0.8	1
85	Morphology of GNAT3â€immunoreactive chemosensory cells in the nasal cavity and pharynx of the rat. Journal of Anatomy, 2021, 239, 290-306.	0.9	1
86	Differences in the expression of catecholamine-synthesizing enzymes between vesicular monoamine transporter 1- and 2-immunoreactive glomus cells in the rat carotid body. Acta Histochemica, 2020, 122, 151507.	0.9	1
87	Immunohistochemical distribution of proteins involved in glutamate release in subepithelial sensory nerve endings of rat epiglottis. Histochemistry and Cell Biology, 2022, 157, 51-63.	0.8	1
88	Distribution of recesses in the olfactory organ of African lungfish <i>Protopterus aethiopicus</i> . Journal of Veterinary Medical Science, 2022, , .	0.3	1
89	Morphological characterization of brush cells in the rat trachea. Tissue and Cell, 2020, 66, 101399.	1.0	0
90	Morphology of <scp>P2X3</scp> â€immunoreactive basketâ€like afferent nerve endings surrounding serosal ganglia and close relationship with vesicular nucleotide transporterâ€immunoreactive nerve fibers in the rat gastric antrum. Journal of Comparative Neurology, 2021, 529, 3866-3881.	0.9	0

#	Article	IF	CITATIONS
91	Effects of CO2 on time-dependent changes in cardiorespiratory functions under sustained hypoxia. Respiratory Physiology and Neurobiology, 2022, 300, 103886.	0.7	0